PERFORMANCE EVALUATION OF THICK CONCRETE SLABS AFFECTED BY ALKALI-SILICA REACTION (ASR) : PART 1 : MATERIAL ASPECTS

Anthony Allard[1]*, Sébastien Bilodeau[1], François Pissot[1], Benoît Fournier[1], Josée Bastien[1], Benoît Bissonnette[1]

[1]Université Laval, Québec, QC, CANADA

Abstract

Concerns have been raised about the structural capacity of aging concrete slabs affected by ASR which reduces the mechanical properties of concrete, influencing the shear resistance mechanisms. As such, a study was carried out to determine the residual shear capacity of thick concrete slabs without stirrup with the progress of ASR. Two sets of three reactive and one non-reactive concrete specimens were fabricated and subjected to conditions conducive to the development of ASR. At selected expansion levels, one concrete specimen from each set was used to characterize the damage occurring within the specimens as it might affect the shear resistance mechanisms. The reduction in rigidity, compressive and tensile strength were evaluated and coupled with the *Stiffness Damage Test* and *Damage Rating Index* to fully evaluate the damage. The results suggest that a strong deterioration gradient is present within the specimens, influenced by the restraining effect of the bottom steel reinforcement.

Keywords: Thick slabs, Deterioration gradient, Damage Rating Index, Stiffness Damage Test.

1 INTRODUCTION

A large number of concrete structures were built in the 1960's to 1970's in North America. Several of them are now subjected to traffic volumes and loads that are way above the standards of the time. This is the case of structures consisting of thick concrete slabs without shear reinforcement that have experienced damage from excessive shear stresses and that needed to be reinforced or replaced. Moreover, some of these structures were found to be affected by pathologies such as alkali-silica reaction, which might have progressively affected their mechanical properties and, potentially, their structural integrity.

Alkali-silica reaction (ASR) is a chemical reaction occurring between reactive siliceous phases and the alkali hydroxides from the concrete pore solution which forms a secondary alkali-silica gel. The reaction products absorb the available water from the pore solution and surrounding environment, thus causing swelling, internal stresses and cracking of the concrete. As demonstrated by multiple authors, ASR will cause a reduction of the mechanical properties of the material [1–3]. While the compressive strength will not be significantly reduced until large levels of expansion are reached, ASR is known to have a strong and rapid impact on the tensile strength and the modulus of elasticity of concrete [4].

A lot of research has been carried out on the evaluation of the potential alkali-reactivity of concrete aggregates and methods of prevention, but comparably few studies or recommendations were done/provided concerning the evaluation of the effect of ASR on the structural performance of concrete structures [5,6]. The knowledge available is still limited and, as such, it remains difficult to provide recommendations on the most appropriate tools for investigating aging concrete structural elements affected by ASR, as well as efficient remedial actions to implement.

Few studies interested in the shear strength of ASR-affected concrete members have been published [7]. Moreover, conclusions vary widely from one study to another, as some of those conclude that ASR has a beneficial effect on the structural capacity while others suggest the opposite. This can be explained by the widely diverging factors adopted between the different studies, such as the reinforcement level, the anchorage of the rebars, the dimensions of the elements studied, the severity of ASR and the type of reactive aggregates used. Hence, a study was carried out in order to contribute to a better understanding of the effect of ASR on the long-term performance of thick concrete slabs without shear reinforcement affected to various degrees by ASR.

* Correspondence to : anthony.allard.1@ulaval.ca

2 OBJECTIVE AND SCOPE OF WORK

This study involves the manufacturing and testing of two sets of four concrete slabs, 610 x 750 x 4500 mm in size, designed with no-shear reinforcement and incorporating a highly-reactive coarse aggregate. Although the dimensions of the above structural elements are closer to that of a beam, they are considered as sections of a one-way slab for the purpose of this study since the width of a slab does not have a significant impact on the cracking profile and on the shear stress [8]. The specimens will consequently be called slabs in the rest of the paper.

The two different sets of slabs include three reactive and one control (non-reactive) slabs; they were subjected to conditions conducive to the development of ASR (high humidity and temperature (38°C) until predetermined (or "cut-off") expansion levels were attained (0.07, 0.15 and 0.23%). For each set, two reactive and the non-reactive slabs were subjected to three-point (flexural) loading in order to evaluate their residual structural capacity in shear (results presented in [9]). The other reactive slabs were reserved for an extensive characterization of the damage induced by ASR. As such, these slabs were exhaustively cored and theses cores submitted to an extensive battery of tests to establish how the ASR has affected the material's properties. These include "conventional" compression, tension and modulus of elasticity determinations, as well as material's detailed characterization through stiffness damage testing (SDT) and semi-quantitative petrographic analysis (*Damage Rating Index* - DRI). The combination of the structural [9] and material testing aspects implemented in this study is expected to contribute to a better understanding of the effect of ASR on the performance of flat slab bridges (i.e. including decks with no shear reinforcement), in particular the link between material's deterioration and its impact on structural integrity, and for developing a model investigation program for the condition assessment of such aging concrete.

3 MATERIALS AND METHODS

3.1 General

While the results of the structural testing performed in this study are presented in [9], this paper focuses on the results of the material's investigations (mechanical properties and microstructural analyses) carried out on two slabs affected to moderate and severe levels by ASR.

As stated above, two sets of four thick concrete slabs were manufactured. The slabs, 610 x 750 x 4500 mm in size (Figures 1 & 2), include flexural reinforcement (1.18%) consisting of ten Canadian 25M rebar [10] at the bottom and three 10M shrinkage-controlling bars in the upper section of the slabs. The steel properties are discussed in [9].

3.2 Materials, mix designs and manufacturing of the concrete slabs

The concrete was formulated in order to promote the development of ASR. The mix designs are presented in Table 1. An ASTM Type I/II high alkali Portland cement (1.12% Na_2O_{eq}) was used as well as a non-reactive granitic sand from Quebec city's greater area. In order to generate an appreciable ASR expansion within a reasonable time frame, a highly reactive coarse aggregate from New Mexico (USA) was selected. It is a polymictic igneous gravel where the reactive phases are mostly composed of volcanic glass and microcrystalline quartz. Its reactivity has been proven by multiple authors over the years [11–13] and an accelerated mortar bar test [14] confirmed it with an expansion of 1.09% at 14 days.

The concrete formulation differs slightly from one set of slabs to another. For the first set, an ASTM C 1293 inspired mix design was used to promote high ASR expansions; however, since the sponsor of the investigation wanted a formulation generating a 28-day compressive strength closer to that used for this type of structure, the cement content was slightly reduced for the second set of slabs (Table 1). In order to promote the development of expansion, external alkalis in the form of NaOH were also added to the reactive concretes to attain a concentration of 1.25% Na_2Oeq by cement mass. A non-reactive reference formula was also used by adding a 30%-solid $LiNO_3$ admixture at 125% of the standard dosage recommended by the manufacturer. This admixture was used since its efficacy in reducing/mitigating the expansion with the reactive aggregate used in this investigation was proven through an extensive laboratory investigation [15].

The concrete mixes were manufactured in a small premix concrete plant. Each mix, of about 2.5 m^3, was made in five batches, each one of them being placed and homogenized in a ready-mixed concrete truck at the plant and during transportation to the university laboratories. The fresh concrete properties (slump, air content and unit weight) of the concrete were measured prior to casting. The concrete was then placed and properly consolidated in the forms, while concrete cylinders, 100 x 200 mm in size, were cast to determine the 28-day compressive strengths.

3.3 Curing and conditioning

The specimens were subjected to seven days of moist curing, demoulded and then installed in a temperature-controlled room with conditions conducive to alkali-silica reaction (38°C, RH > 95% (Figure 2A)). In order to keep the specimens in a high level of humidity, a pierced water hose was installed over the slabs and these were enclosed in a "tent" system made of impermeable polyethylene tarps (Figure 2B).

3.4 Monitoring of expansion

In order to monitor the length variation of the concrete specimens, the latter were equipped with stainless steel studs; however, the surface arrangement of the studs was slightly changed for the second set of slabs in order to get a more complete coverage of the expansion occurring within the reactive concrete elements (Figures 3 & 4). These studs were embedded by drilling and fixed with an epoxy adhesive on three faces of each slab in order to monitor the longitudinal, transversal and vertical ASR induced expansion. The length variations were regularly monitored using a Mayes extensometer, while the temperature of the storage room was lowered to 23°C for 24 hours prior to the measurements. Welded strain gages were also installed on some of the rebars of the 2nd set of slabs to assess the importance of the "chemical prestressing".

3.5 Methods for assessment and analysis

General

The conditioning of the specimens was maintained until predetermined expansion levels were reached. The expansion criterion was determined to be the central longitudinal expansion on the top face of the slabs. When the cut-off criterion was reached (i.e. 0.07, 0.15, 0.23-0.24%), two reactive slabs and the non-reactive one from each set were subjected to a structural testing program [9]. The remaining reactive slab of each set was used to perform full material's condition assessment, which is the topic of this paper.

In order to evaluate the damage induced by ASR, the slabs were subjected to extensive coring (Figure 5). This coring plan allowed evaluating the condition of concrete within the whole volume of the elements, especially to determine if the direction of coring (horizontal or vertical) has an effect on the test results. Considering the symmetry of the slab's detailing, cores were extracted horizontally on one side and vertically on the other side. Horizontal cores were taken at three elevations/levels from the side of the slabs (A, B, C on the left end side of Figure 5), while vertical cores were taken in three different rows from the top of the slabs (D, E, F on the right end side of Figure 5). For the purpose of this paper, only the results obtained from the horizontal cores will be presented. As illustrated on the left end side of Figure 5B, horizontal coring was done across the whole thickness of the slab (i.e. 610 mm), thus allowing to obtain three specimens from each cores for further testing. Cores from the columns, 1, 4, 7 and 10 were reserved for the SDT and compression, while the cores from columns 2, 5, 8, 11 were used for the tensile testing. The cores from the leftover columns were used for the DRI.

The non-reactive slabs were reserved for structural testing, but they were also cored afterwards to serve as a reference level for comparing the severity in ASR-damaged concretes. The cores were obtained from the extremities of the slabs where minimal damage resulted from structural testing.

Strength testing

The compressive strength and the splitting tensile strength of the concrete were evaluated at three depths on multiple 100 mm diameter cores. The latter is an indirect method to obtain the tensile strength, while the «pure» tensile strength is estimated to be around 65% of the splitting tensile strength[16].

Stiffness Damage Test

The *Stiffness Damage Test* (SDT) is a cyclical compression test first introduced by Crouch [17]. A concrete core or cylinder is submitted to five cycles of loading-unloading at a rate of 0,1 MPa/sec. The specimen is inserted in a metallic cage instrumented with linear variable differential transformers (LVDT) registering the deformations within the specimen during the cycles. Many changes have been proposed over the years to this test, but the method used in this study is the one proposed by Sanchez [4] where the maximum load used for testing represents 40% of the undamaged concrete's compressive strength. The *Stiffness Damage Index* (SDI) is the output parameter used in this study since it provides interesting information concerning the magnitude of cracking affecting the material. The SDI represents the ratio between the dissipated energy and the total energy developed during the test.

The *Stiffness Damage Test* also allows obtaining concrete's modulus of elasticity, as the average of that obtained during the 2nd and 3rd cycles [18,19]. This parameter will provide important information concerning the effect of ASR on the rigidity of the material.

Damage Rating Index (DRI)

The *DRI* is a semi-quantitative petrographic analysis of a polished concrete section. This analysis is particularly interesting as it quantifies the presence of petrographic features of ASR and multiples studies have shown that it is able to reliably evaluate the advancement of the reaction[11,20,21]. A grid of 1 cm by 1 cm is traced on the finely polished surface and a minimum of 150 cm² is examined through the use of a stereobinocular microscope at a magnification of 15X. The examination consists in counting the petrographic features associated with ASR and multiplying the sum of the counts by specific weighing factors. The total sum is then normalized for a surface area of 100 cm², which provides the DRI number. The petrographic features and the weighing factors used in this study are those proposed by Villeneuve [22] and are presented in Table 2.

4 RESULTS

Properties of fresh and hardened concrete

The properties of fresh and hardened concrete are presented in Table 3. Higher slumps and lower 28-day compressive strengths were obtained for the second set of slabs.

Expansion

The "cut-off" expansion reached by the four slabs referenced in this paper are presented in Table 4; it represents the central longitudinal expansion on the top face of each slab. However, the deformations measured were found to be very heterogeneous. The range of expansions obtained for the slab 2-R3 is shown in Figures 6, 7 and 8. At the end of the 55-week high-humidity storage, the longitudinal expansion for the top face of the slab ranged from 0.20 to 0.30%, while the transversal expansion is two to three times more important, ranging from 0.60 to 0.70% (Figure 6). The vertical expansions registered on the side face of 2-R3 ranged from 0.13 to 0.21% (Figure 8), the lowest values being generally obtained towards the ends of the slabs (i.e. closer to the reinforcing bars – Figure 1). Figure 7 shows that the longitudinal expansion is much more important at the top than in the bottom part of the slab.

Mechanical properties

The mechanical properties (average compressive and tensile strength values) of the non-reactive cores are shown in Table5. The average compressive strengths of 1-NR and 2-NR are 47.9 MPa and 44.3 MPa, respectively, with coefficients of variation less than 10%. The average tensile strength is 2.5 MPa for 1-NR and 2.3 MPa for 2-NR, with coefficient of variation slightly higher than 10 %. The modulus of elasticity is respectively 32.3 and 33.3 GPa for 1-NR and 2-NR, presenting low variability (about 4%).

The mechanical properties obtained for both reactive slabs are presented in Table 6 and 7. The average compressive strength, tensile strength and modulus of elasticity values are presented at three different heights (from the bottom of the slab), level A being the highest (600mm) and C the lowest (210 mm). The strengths are always higher for cores of 1-R2 than the ones from 2-R3, which is consistent with the change in mix design and the highest expansion level reached by slab 2-R3. The average compressive strengths vary from 34.6 to 46.1 MPa and from 28.3 to 35.5 MPa for 1-R2 and 2-R3, respectively, with horizontal average values of 39.6 for 1-R2 and 31.5 for 2-R3. The average tensile strengths vary from 1.6 to 2.2 for 1-R2 with a horizontal average of 1.8 MPa, while 2-R3's average tensile strengths ranged from 1.3 to 1.8 MPa with a horizontal average of 1.6 MPa.

The moduli of elasticity were also determined and ranged from 17.6 GPa (upper part) to 27.1 GPa (lower part) of slab 1-R2. The slab 2-R3 showed lower results with moduli ranging from 14.0 (upper part) to 20.6 GPa (lower part). The horizontal average moduli of elasticity are of 21.5 and 17.2 GPa for 1-R2 and 2-R3, respectively.

The results presented here are the average for each depths of the cores extracted horizontally within the slabs. However, the results presented for the non-reactive slabs are the average of all the cores tested regardless of their orientation since less cores were tested.

Stiffness Damage Test (SDT)

The *SDT* provides useful output parameters with one of the most interesting being the *Stiffness Damage Index (SDI)*. The lower the SDI, the less cracking there is within the material.

The global average SDI for the non-reactive slabs 1-NR and 2-NR were respectively of 0.10 and 0.11, as shown in Table5. However, the SDI of the reactive slab 1-R2 ranged from 0.37 for the higher horizontal cores to 0.19 for the lowest with a global average of 0.29 (Table 6). The slab 2-R3 generated SDIs ranging from 0.38 at the upper to 0.26 at the lower level, with a global average of 0.30 (Table 7).

Damage Rating Index

The Damage Rating Index is quite useful from a materials point of view as it can provide clues which might explain reductions in mechanical properties or in rigidity of an ASR affected concrete. The DRI was performed at three levels for the cores extracted horizontally (full widths of 610 mm). The horizontal DRI results are illustrated in Figure 9 for slabs 1-R2 and 2-R3. The DRI results for slab 1-R2 range from about 700 in the upper level to about 300 in the bottom of the slab. The DRI results for the second slab are much higher, as they range from about 1200 at the top to about 700 at the bottom. This seems to indicate that a much higher level of cracking was present in the cores from slab 2-R3 presenting a higher level of expansion.

5 DISCUSSION

Expansion

The monitoring of the reactive slabs indicated a clear expansion trend from the bottom towards the upper part of the specimens, reaching maximum expansions (0.6-0.7%) in the transverse direction (slab 2-R3 - Figure 6). This can be attributed to the presence of an important quantity of flexural steel bars in the bottom part of the slabs, where they largely restrain the expansive pressure generated by ASR. However, as the distance increases from that rebar layer, this confining effect progressively vanishes to reach somewhat "free expansion" conditions towards the upper part of the concrete element. A representation of the expansive behaviour occurring within the slabs is given in Figure 10. The above expansive behaviour was accompanied by extensive surface cracking, with cracking density and crack openings increasing toward the upper part of the slabs, as illustrated in Figures 11 & 12.

Stiffness Damage Test (SDT) and the Stiffness Damage Index (SDI)

The SDI provides information regarding the magnitude of cracking inside the materials, as it represents the ratio of the energy consumed for «closing» the cracks in the concrete specimen on the total energy implemented in the system.

The low SDI values obtained for the non-reactive slabs suggest that the concrete possesses only few defects, thus confirming that the $LiNO_3$efficiently mitigated the ASR (Table 5). On the other hand, the analysis of the SDI values for both reactive slabs indicates that the magnitude of cracking varies according to the height of the specimens, with lower SDIs at the base of both slabs and higher SDIs at the top. It is interesting to note that even though slab 2-R3 exhibits a higher degree of expansion compared to 1-R2, it did not have an important impact on the maximum SDI as both slabs generated similar maximum SDI values (0.37 vs 0.38). However, there is a difference in the internal concrete damage according to the height, with slab 2-R3 presenting a smaller variation in SDIs (0.26 to 0.38) compared to slab 1-R2 (0.19 to 0.37). This indicates that more damage was induced by ASR in the bottom part of the second set of slabs but that the reinforcement was capable of restraining expansion in the lower part of the specimens. It also indicates that after a certain expansion level, the SDI values might level off which would corroborate the observations of Sanchez [4] that are attributed to the presence of large amounts of alkali-silica gel in the cracks as the ASR expansion increases.

It is also interesting to note that the SDI exhibits a high variability for specimens that were taken in the same zones (depths). Indeed, the coefficients of variation are quite high, varying from 11 to 34 % for slab 1-R2 and 13% to 22% for slab 2-R3. This suggests that the defects induced by ASR display a great level of heterogeneity, and that it might sometimes be difficult to establish a difference between the levels studied. However, the difference between level A and C establishes concrete evidence of a deterioration gradient within the slabs.

Damage Rating Index

The petrographic features identified in the polished concrete cores are physical manifestations of ASR damage. As illustrated in Figure9, the farthest the cores are from the layer of rebar, the higher is the DRI value. This indicates that the damage induced by the reaction increases with height in the slabs, thus confirming the results of SDI. Interestingly, a similar degree of damage (i.e. similar DRIs) is obtained in the bottom part of slab 2-R3 and in the upper part of slab 1-R2 despite very different

expansion levels (0.05% vs 0.12%), thus suggesting that the presence of reinforcement can restrain ASR expansion without necessarily reducing the development of internal damage (cracking) due to ASR.

A closer analysis of the petrographic features of deterioration in Figure 9 indicates that the increasing trends in DRI values with increasing heights in the slabs are mostly caused by the increasing magnitude of cracking with secondary reaction products within the coarse aggregate (Cr+RPCA) and the cement paste (Cr+RPCP). The cracks containing reaction products in the cement paste increase with the height of the specimen for both slabs, but it is the most important petrographic feature of deterioration in slab 2-R3. This would support the hypothesis proposed by Sanchez [4] that the increasing presence of alkali-silica gel in cracks mitigates the increase in SDI values with increasing expansion due to ASR.

Mechanical properties

Comparing the mechanical properties of the reactive and non-reactive cores allows determining the deleterious effect of ASR on material's properties. The reduction in compressive and tensile strength increase with the height for both sets of slabs, as seen in Table 6 and 7. The reduction in compressive strength are more important for the slab displaying a higher level of expansion, as it ranges from 3.7 to 27.8 % for 1-R2 and from 20 to 36.1% for 2-R3. The same phenomenon is observed for tensile strength, with reductions ranging from 8.9 % at the base of the slab to 32.8% at the top for 1-R2, while 2-R3's tensile strengths display a decrease varying from 23.3% at the bottom to 43.8% at the higher level. Interestingly, the tensile and compressive strengths display limited variability, with coefficients of variation mostly lower than 10%. Both slabs present higher losses in modulus of elasticity in the higher level (45.6 % for 1-R2 and 57.9 for 2-R3) compared to the zone closer to the flexural reinforcement (16.2% for 1-R2 and 20.6% for 2-R3). The variability in moduli of elasticity is low for 1-R2 (about 10%) while more important for 2-R3 (up to 23.2%).

These losses in mechanical properties can be explained with the help of the SDI and DRI values, which showed that an important cracking network induced by ASR is present within the concrete. Also, this cracking network shows an important gradient that is largely influenced by presence of the steel reinforcement located at the bottom and along the sides of the slabs (Figure 1). The presence of that reinforcement in the bottom part of the slab, although not sufficient to eliminate ASR-induced cracking, induces a restraining effect on expansion in that portion of the slab which vanishes with increasing heights, thus explaining the higher losses in mechanical properties and higher SDI and DRI towards the top of the slabs.

6 CONCLUSIONS

A detailed condition assessment of thick concrete slabs without shear reinforcement and affected to different degrees by ASR was carried out. Significant reductions in mechanical properties, reaching 36% for the compressive strength, 44% for the tensile strength and 58% for the modulus of elasticity were observed. The above reductions were however found to vary largely according to the distance from the reinforcement. Actually, although the confining effect of the steel reinforcement can greatly affect the expansions/ deformations of the concrete, it will not necessarily mitigate the development of ASR cracking or the material's damage. Such a damage gradient within the structural element can be highlighted through mechanical testing (tensile strength and modulus of elasticity, SDT) and semi-quantitative petrographic analysis (DRI).However, the extent of material's damage is not necessarily a direct indication of the structural performance of the element, as is demonstrated in part II [9].

7 ACKNOWLEDGEMENTS

The funding of this project was provided by a grant from the Quebec Department of Transportation, under the supervision of Mr. Daniel Boulet and Mrs. Kim Lafrance.

8 REFERENCES

[1] Fournier, B, Bérubé, MA, Alkali-aggregate reaction in concrete: a review of basic concepts and engineering implications, Canadian Journal of Civil Engineering. 27 (2000) 167–191.

[2] Pleau, R, Bérubé, MA, Pigeon, M, Fournier, B, Raphaël, S, Mechanical behavior of concrete affected by ASR, in: Conf. Proc. 8th ICAAR. 1989: pp. 721–726.

[3] Clayton, N, Currie, RJ, Moss, RM, The effects of alkali-silica reaction on the strength of prestressed concrete beams, The Structural Engineer. 68 (1990) 287–292.

[4] Sanchez, LFM, Contribution to the assessment of damage in aging concrete infrastructures

affected by alkali-aggregate reaction, Ph.D. Thesis, Université Laval, 2014.
[5] Maltais, Y, Paradis, F, Évaluation de la capacité portante des ponts routiers sans armatures de cisaillement affectés par la réaction alcalis-silice, in: Congrès Annuel SCGC, 2008: pp. 1–19.
[6] CUR - Recommandation 102, Inspection and assessment of concrete structures in which the presence of ASR is suspected or has been established, CUR, Gouda, 2008.1–31.
[7] den Ujil, JA. Structural consequences of ASR: an example on shear capacity, Heron. 47 (2002) 125–139.
[8] Sherwood, EG, Lubell, AS, Bentz, EC, Collins, MP, One-way shear strength of thick slabs and wide beams, ACI Structural Journal. 103 (2006) 794–802.
[9] Bilodeau, S, Allard, A, Bastien, J, Pissot, F, Fournier, B, Mitchell, D, Bissonnette, B, Performance Evaluation of Thick Concrete Slabs Affected by Alkali-Silica Reaction (ASR) - Part II: Structural Aspects, in: Conf. Proc. 15th ICAAR, Sao Paulo, Brasil, 2016.
[10] Canadian Standards Association, CSA G30.18-09 : Carbon steel bars for concrete reinforcement, (R2014) 1–14.
[11] Villeneuve, V, Fournier, B, Duchesne, J, Determination of the damage in concrete affected by ASR - the damage rating index (DRI), in: Conf. Proc. 14th ICAAR, 2012.
[12] Fournier, B, Ideker, J, Folliard, KJ, Thomas, MDA, Nkinamubanzi, PC, Chevrier, R, Effect of environmental conditions on expansion in concrete due to alkali–silica reaction (ASR), Materials Characterization. 60 (2009) 669–679.
[13] Smaoui, N, Bérubé, MA, Fournier, B, Bissonnette, B, Durand, B, Evaluation of the expansion attained to date by concrete affected by alkali–silica reaction. Part I: Experimental study, Canadian Journal of Civil Engineering. 31 (2004) 826–845.
[14] Canadian Standards Association, CSA A23.2-25A: Test method for detection of alkali-silica reactive aggregate by accelerated expansion of mortar bars, in: CSA A23.2 Test Methods & Standard Practice in Concrete, Mississauga, Ontario, Canada, 2014: pp. 425–433.
[15] Fournier, B, Thomas, MDA, Folliard, KJ, Nkinamubanzi, PC, Chevrier, R, Borborak, et al., Use of lithium in fresh concrete to prevent deleterious expansion due to ASR, Federal Highway Administration (USA), Lithium Technology Research Studies and Reports for Mitigation of ASR in Concrete, 2011. 400p.
[16] Massicotte, B, Calcul des structures en béton armé: concepts de base, Les Éditions da Vinci, 2013, 353p.
[17] Crouch, RS, Specification for the determination of stiffness damage parameters from the low cyclic uniaxial compression of plain concrete cores. Revision A, Mott, Hay & Anderson, Special services division, Internal technical note 1987.
[18] Sanchez, LFM, Fournier, B, Jolin, M, Bastien, J, Evaluation of the Stiffness Damage Test (SDT) as a tool for assessing damage in concrete due to alkali-silica reaction (ASR): Input parameters and variability of the test responses, Construction & Building Materials. 77 (2015) 20–32.
[19] Sanchez, LFM, Fournier, B, Jolin, M, Bastien, J, Evaluation of the stiffness damage test (SDT) as a tool for assessing damage in concrete due to ASR: Test loading and output responses for concretes incorporating fine or coarse reactive aggregates, Cement & Concrete Research. 56 (2014) 213–229.
[20] Rivard, P, Ballivy, G, Assessment of the expansion related to alkali-silica reaction by the Damage Rating Index method, Construction & Building Materials. 19 (2005) 83–90.
[21] Sanchez, LFM, Fournier, B, Jolin, M, Duchesne, J, Reliable quantification of AAR damage through assessment of the Damage Rating Index (DRI), Cement & Concrete Research 67 (2015) 74–92.
[22] Villeneuve, V, Détermination de l'endommagement du béton par méthode pétrographique quantitative, M.Sc. Thesis. Université Laval, 2011.

9 TABLES AND FIGURES

TABLE 1: Mix designs used for the reactive and non-reactive slabs used for material's investigations.

Set	*Mix no.*	*Cement (kg/m³)*	*Fine Aggregate (SSD) (kg/m³)*	*Coarse Aggregate (SSD) (kg/m³)*	*Hydration water* (kg/m³)*	*Water-to-cement ratio*	*$LiNO_3$ (Liters)*	*NaOH (kg)*
1	1-NR	420	770	1016	199	0.47	27	---
	1-R2	420	770	1016	204	0.49	---	---
2	2-NR	370	714	1073	174	0.47	23.6	---
	2-R3	370	714	1073	174	0.47	---	0.699

TABLE 2: Petrographic features identifies for the DRI and their corresponding factors proposed by Villeneuve [22].

Petrographic features	**Weighing Factors**
Closed cracks in coarse aggregate (CrCA)	0,25
Opened cracks in coarse aggregate (OCrCA)	2
Cracks in coarse aggregate with reaction product (Cr+RPCA)	2
Coarse aggregate debonded (CAD)	3
Coarse aggregate corroded (CAC)	2
Cracks in cement paste (CrCP)	3
Cracks with reaction product in cement paste (Cr+RPCP)	3

TABLE 3: Properties of fresh and hardened concrete.

Set	Slab	Unit weight (kg/m³)	Slump (mm)	Air content (%)	f'_c (Mpa) 28 days
1	1-NR	2370	50	2.2	46.8
	1-R2	2349	100	1.8	41.0
2	2-NR	2371	205	1.6	34.4
	2-R3	2379	185	1.4	34.4

TABLE 4: Slabs' expansions as defined by the cut-off criterion (central longitudinal expansion on the top face of the slabs)

Set	*Slab*	*Expansion*
1	1-NR	0.01 %
	1-R2	0.14 %
2	2-NR	0.01 %
	2-R3	0.23%

TABLE 5: Material's testing results for the non-reactive slabs. CV represents the coefficient of variation and (*n*) is the number of specimens tested.

Set	Slab	f'_c(MPa)	CV (%) (*n*)	f'_t(MPa)	CV (%) (*n*)	E (GPa)	CV (%) (*n*)	SDI	CV (%) (*n*)
1	1-NR	47.9	9.6 *(29)*	2.5	12.4 *(30)*	32.3	4.0 *(29)*	0.11	9.4 *(29)*
2	2-NR	44.3	6.7 *(19)*	2.3	11.8 *(10)*	33.3	4.4 *(14)*	0.10	15 *(14)*

TABLE 6: Material results for the horizontal cores of slabs 1-R2. (*x*) is the reduction in mechanical properties compared to the respective non-reactive slab, CV is the coefficient of variation and (*n*) is the number of specimens tested.

Slab 1-R2									
Orientation	Position	Compressive strength		Tensile strength		Modulus of elasticity		Stiffness Damage Index	
		f'_c(MPa) *(x)*	CV (%) (*n*)	f'_t(MPa) *(x)*	CV (%) (*n*)	E (GPa) *(x)*	CV (%) (*n*)	SDI	CV (%) *(n)*
Horizontal	Level A (600 mm)	34.6 *(27.8)*	5.6 *(8)*	1.6 *(32.8)*	7.9 *(10)*	17.6 *(45.6)*	7.0 *(9)*	0.37	11.3 *(9)*
	Level B (405 mm)	37.2 *(22.3)*	5.3 *(10)*	1.8 *(25.9)*	7.8 *(10)*	19.5 *(39.7)*	8.8 *(11)*	0.31	15.1 *(11)*
	Level C (210 mm)	46.1 *(3.7)*	7.0 *(10)*	2.2 *(8.9)*	9.3 *(6)*	27.1 *(16.2)*	11.7 *(10)*	0.19	34.4 *(10)*
Horizontal average		39.6 *(17.2)*	14.1 *(28)*	1.8 *(24.7)*	14.7 *(26)*	21.5 *(33.5)*	21.7 *(30)*	0.29	31.1 *(30)*

TABLE 7: Material results for the horizontal cores of slabs 2-R3. (*x*) is the reduction in mechanical properties compared to the respective non-reactive slab, CV is the coefficient of variation and (*n*) is the number of specimens tested.

Slab 2-R3									
Orientation	Position	Compressive strength		Tensile strength		Modulus of elasticity		Stiffness Damage Index	
		f'_c(MPa) *(x)*	CV (%) (*n*)	f'_t(MPa) *(x)*	CV (%) (*n*)	E (GPa) *(x)*	CV (%) (*n*)	SDI	CV (%) (*n*)
Horizontal	Level A (600 mm)	28.3 *(36.1)*	9.6 *(11)*	1.3 *(43.8)*	9.6 *(8)*	14.0 *(57.9)*	23.2 *(11)*	0.38	22.4 *(11)*
	Level B (405 mm)	30.2 *(31.9)*	9.2 *(11)*	1.6 *(32.6)*	7.9 *(9)*	16.8 *(49.4)*	15.9 *(12)*	0.29	15.5 *(12)*
	Level C (210 mm)	35.5 *(20.0)*	8.3 *(12)*	1.8 *(23.3)*	12.6 *(9)*	20.6 *(38.1)*	8.1 *(12)*	0.26	12.5 *(12)*
Horizontal average		31.5 *(29.0)*	13.1 *(34)*	1.6 *(32.8)*	16.2 *(26)*	17.2 *(48.2)*	21.5 *(35)*	0.30	24.6 *(35)*

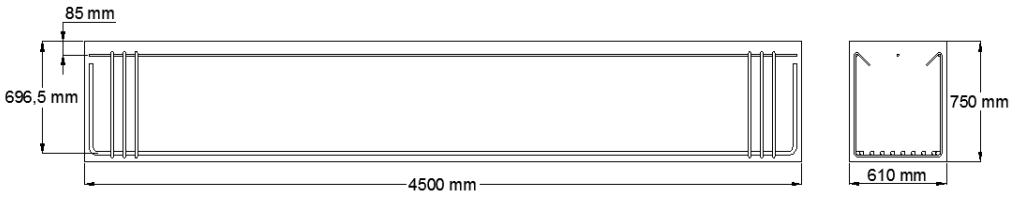

FIGURE 1: Design of the concrete slabs.

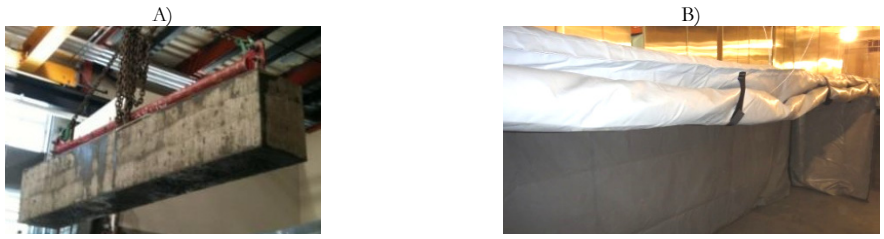

FIGURE 2: A. Concrete slab transported to the temperature-controlled room. B. Large tarp used to maintain high humidity conditions surrounding the slab.

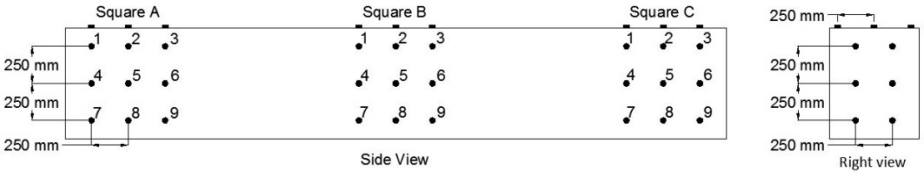

FIGURE 3: Studs locations for the expansion monitoring for the first set of slabs.

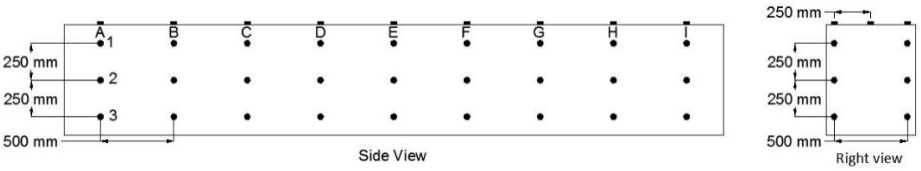

FIGURE 4: Studs location for the expansion monitoring for the second set of slabs.

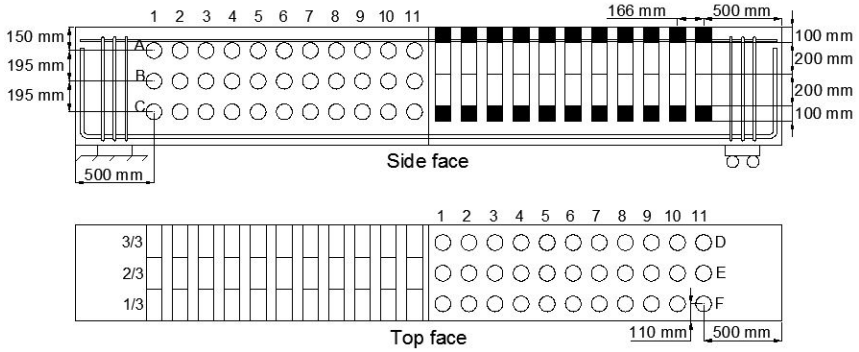

FIGURE 5: Coring plans for slabs 1-R2 and 2-R3. The test results reported in this paper are for cores extracted horizontally, i.e. corresponding to the left portion of the sketches above.

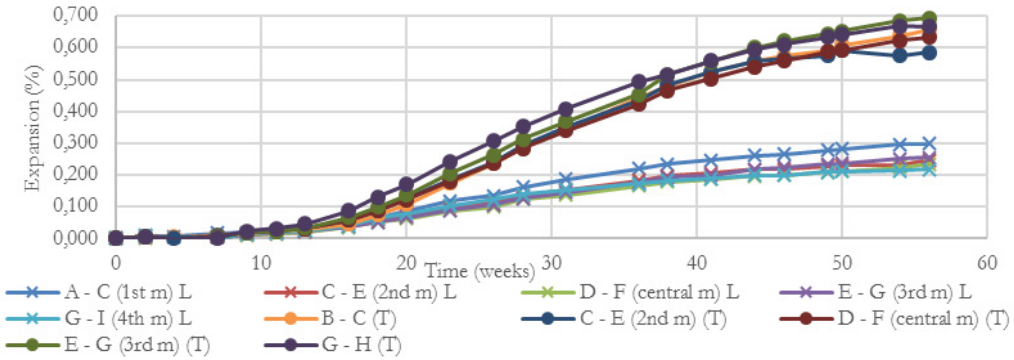

FIGURE 6: Longitudinal (L) and Transversal (T) expansions on the top face of slab 2-R3. For example, the value given for A-C (1st m) L is the average of the longitudinal measurements obtained for columns A through C on the top face (Figure 4).

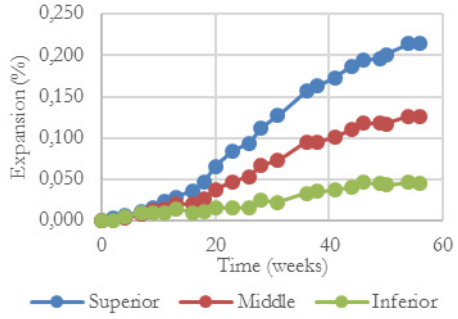

FIGURE 7: Average longitudinal expansions on the side face of slab 2-R3.

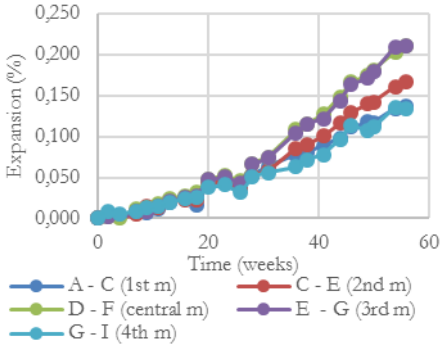

FIGURE 8: Average vertical expansion on the side face of slab 2-R3. For example, the value given for A-C (1st m) is the average of the vertical measurements obtained for columns A through C (Figure 4).

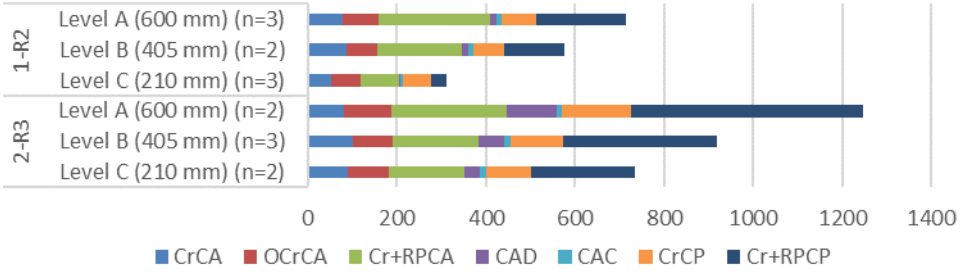

FIGURE 9: Damage Rating Index results for each height in both reactive slabs. The explanation for the abbreviations can be found in TABLE 2 while *n* is the number of cores tested.

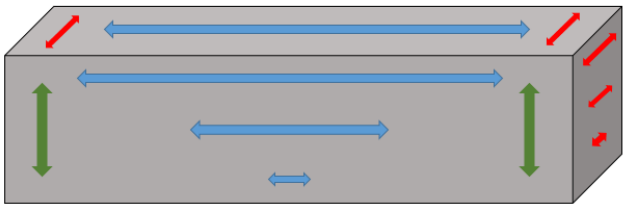

FIGURE 10: Representation of the expansion occurring within the slabs.

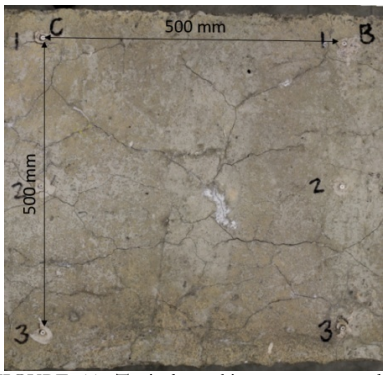

FIGURE 11: Typical cracking present on the top face of slab 2-R3.

FIGURE 12: Cracking on the upper surface of slab 2-R3 highlighted with black marker.